

# Criticality in the two-dimensional random-bond Ising model

Sora Cho

*Department of Physics, University of California, Santa Barbara, California 93106*

Matthew P. A. Fisher

*Institute for Theoretical Physics, University of California, Santa Barbara, California 93106*

*and Department of Physics, University of California, Santa Barbara, California 93106*

(Received 25 July 1996)

The two-dimensional (2D) random-bond Ising model has a novel multicritical point on the ferromagnetic to paramagnetic phase boundary. This random phase transition is one of the simplest examples of a 2D critical point occurring at both finite temperatures and disorder strength. We study the associated critical properties, by mapping the random 2D Ising model onto a network model. The model closely resembles network models of quantum Hall plateau transitions, but has different symmetries. Numerical transfer matrix calculations enable us to obtain estimates for the critical exponents at the random Ising phase transition. The values are consistent with recent estimates obtained from high-temperature series. [S0163-1829(97)00902-8]

## I. INTRODUCTION

Two-dimensional 2D models have played a special role in the theory of phase transitions.<sup>1</sup> In 1944 Onsager's exact solution of the 2D Ising model gave critical exponents that were simple rational numbers, although different than Landau theory. In the 1970 renormalization group (RG) calculations revealed exponents varying continuously below an upper critical dimension, illustrating the breakdown of Landau theory. But it was unclear why the 2D Ising exponents and those for other exactly soluble 2D models were rational numbers. This fact was explained by the remarkable development of conformal field theory in the 1980s. Under the assumption of conformal invariance at criticality, it was possible to analyze a large class of 2D critical points.<sup>1</sup> Moreover, a first step was made towards a full classification of *all* allowed 2D phase transitions.

Many physically important 2D phase transitions occur in systems with quenched disorder. An example of particular experimental interest is the transition between plateaus in the integer quantum Hall effect (IQHE).<sup>2</sup> This transition has been successfully studied numerically, but so far has eluded analytic treatments via either RG calculations, exact methods or conformal field theory. Given the general power of conformal field theory in 2D, it has been surprisingly unhelpful in understanding such random phase transitions.

In this paper we analyze a nontrivial 2D random phase transition which occurs in the simplest of all models: the 2D Ising model with random bonds. Our approach is numerical, and closely parallels earlier work on the IQHE transition.<sup>2</sup> We first map the 2D random Ising model into a variant of the Chalker-Coddington<sup>3</sup> network model, which describes non-interacting chiral fermions. The random Ising transition corresponds to a fermion localization transition. We extract critical exponents numerically by standard transfer matrix methods. The values are in reasonable agreement with those recently obtained by Singh and Adler<sup>4</sup> via high-temperature series. Unfortunately, this random Ising transition has also eluded any analytic treatment.

To be more specific, consider the Ising model on a 2D square lattice,

$$H_J = - \sum_{\langle i,j \rangle} J_{ij} S_i S_j, \quad (1.1)$$

with nearest-neighbor interactions  $J_{ij}$  taken as random variables with a distribution  $P_J(J_{ij})$ . For the simple distribution  $P_J(J_{ij}) = p \delta(J_{ij} + J) + (1-p) \delta(J_{ij} - J)$ , corresponding to a fraction  $p$  of antiferromagnetic bonds, the phase diagram, as established by various methods,<sup>5,6</sup> is shown schematically in Fig. 1.

For small  $p$  there is a phase boundary separating the ferromagnetically ordered phase at low temperatures from the paramagnet. A larger  $p$  destroys the ferromagnetic phase, replacing it in high dimensions ( $d \geq 3$ ) by a spin glass phase. In this case a multicritical point is expected at the coexistence point of all three phases. In 2D the spin glass phase is not present at  $T \neq 0$ , being destroyed by thermal

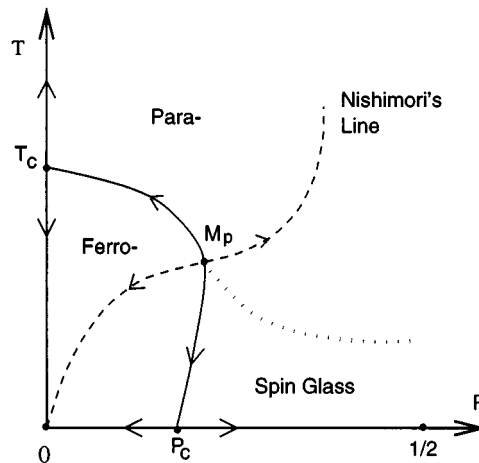


FIG. 1. Schematic phase diagram of the 2D  $\pm J$  random-bond Ising model.

fluctuations.<sup>5</sup> However, the multicritical point still exists on the ferro-to-para phase boundary.<sup>7</sup> The multicritical point is unstable along the phase boundary, with RG flows as depicted in Fig. 1, consistent with the (marginal) irrelevance of weak disorder at the pure 2D Ising critical point ( $p=0$ ). LeDoussal and Harris<sup>8</sup> have argued that the Nishimori line, along which the internal energy is analytic,<sup>9</sup> passes through the multicritical point and coincides with one of the two RG scaling axes. The other scaling axis is tangent to the ferro-to-para phase boundary. Recently, Singh and Adler<sup>4</sup> have obtained estimates for the two associated critical exponents, using a high-temperature series method. From a general point of view, this multicritical point is of interest, being probably the simplest 2D critical point which occurs at both finite temperature and finite disorder strength.

Our paper is organized as follows. In Secs. II and III, we show that the random-bond 2D Ising model can be mapped, using a fermionic representation, to a variant of the Chalker-Coddington network model.<sup>3</sup> This mapping reveals a close similarity between the random Ising transition and the IQHE plateau transition. However, due to a symmetry difference, the two transitions are *not* in the same universality class. In Sec. IV, we employ a transfer matrix approach to analyze the network model, and obtain estimates for the exponents at the random Ising multicritical point. Section V gives a brief summary and conclusion.

## II. FERMIONIC REPRESENTATION

It is well known that the critical properties of the pure 2D Ising transition are equivalent to a massless Majorana (real) fermion field.<sup>1</sup> In his studies of the bond-diluted Ising model, Shankar<sup>10</sup> constructed a model in terms of conventional (Dirac) fermions, by adjoining two identical copies. For the random-bond Ising model, we show below that this procedure leads to a model of 2D chiral fermions, with a hopping matrix element of random *sign*.

Following Shankar,<sup>10</sup> we consider a spatially anisotropic Ising model, retaining a lattice in one direction, but taking the continuum limit in the other (the “imaginary time” direction). The partition function, when expressed in terms of a transfer matrix, can then be written  $Z = \text{Tr} \exp(-\beta H_{1D})$ , where  $H_{1D}$  is a 1D quantum Hamiltonian and  $\beta$  is the system size in the “time” direction. The appropriate 1D Hamiltonian for the pure Ising model is

$$H_{1D} = \sum_n [\kappa_1 \sigma_n^x + \kappa_2 \sigma_n^z \sigma_{n+1}^z], \quad (2.1)$$

where  $n$  label sites of a 1D lattice and  $\sigma^\alpha$  with  $\alpha = x, y, z$  are Pauli matrices. This model exhibits a phase transition when  $\kappa_1 = \kappa_2$ , which is in the (pure) Ising universality class, as verified below. The transition also follows from a duality symmetry which exchanges high- and low-temperature phases.<sup>1</sup> With the definition  $\sigma_n^x \equiv \mu_n^x \mu_{n+1}^x$  and  $\sigma_n^z \equiv \prod_{m < n} \mu_m^z$  the Hamiltonian can be written in the form (2.1) with  $\sigma^\alpha \rightarrow \mu^\alpha$  and  $\kappa_1 \leftrightarrow \kappa_2$ .

The partition function is also invariant under  $\kappa_i \rightarrow -\kappa_i$  ( $i=1,2$ ), as seen by a spin rotation,  $\sigma_n^\alpha \rightarrow -\sigma_n^\alpha$ , with  $\alpha = x, y$  for  $n$  odd and  $\alpha = x, z$  for  $n$  even, which restores the Hamiltonian to its original form. This transformation is

equivalent to  $J \rightarrow -J$  in Eq. (1.1), mapping from a ferromagnetic to antiferromagnetic spin model. Thus randomness in the sign of the exchange interaction in Eq. (1.1) is equivalent to randomness in the *sign* of  $\kappa_i$ . To describe the  $\pm J$  Ising model, we thus consider interactions which are random functions of both  $n$  and imaginary time  $\tau$ ,  $\kappa_i \rightarrow \kappa_i(n, \tau)$ , taking either sign.

A fermionic representation can be obtained by introducing the Majorana fields

$$\eta_1(n) \equiv \frac{1}{\sqrt{2}} \prod_{m < n} \sigma_m^x \sigma_n^y, \quad \eta_2(n) \equiv \frac{1}{\sqrt{2}} \prod_{m < n} \sigma_m^x \sigma_n^z, \quad (2.2)$$

which anticommute,  $\{\eta_i(n), \eta_j(m)\} = \delta_{ij} \delta_{nm}$ . The Hamiltonian is quadratic when expressed in terms of these new variables,

$$H_{1D} = (-2i) \sum_n [\kappa_1 \eta_1(n) \eta_2(n) - \kappa_2 \eta_1(n) \eta_2(n+1)]. \quad (2.3)$$

An identical copy of the system is constructed by introducing a new set of Majorana fields  $\xi_i$ . The Hamiltonian obtained by summing the two,  $\tilde{H} \equiv 1/2 [H_{1D}(\eta_i) + H_{1D}(\xi_i)]$ , can be expressed in terms of standard (Dirac) Fermion operators

$$\psi_i \equiv \frac{1}{\sqrt{2}} (\eta_i + i \xi_i), \quad \psi_i^\dagger \equiv \frac{1}{\sqrt{2}} (\eta_i - i \xi_i) \quad (2.4)$$

as

$$\begin{aligned} \tilde{H} = & \sum_n (-i \kappa_1) [\psi_1^\dagger(n) \psi_2(n) - \psi_2^\dagger(n) \psi_1(n)] + (i \kappa_2) \\ & \times [\psi_1^\dagger(n) \psi_2(n+1) - \psi_2^\dagger(n+1) \psi_1(n)]. \end{aligned} \quad (2.5)$$

Notice that  $\tilde{H}$  has a conserved U(1) charge:  $\psi_1^\dagger \psi_1 + \psi_2^\dagger \psi_2$ . At the pure Ising transition, there are gapless excitations in this conserved charge. With disorder present, the transition corresponds to a localization transition of these conserved fermions.

To complete the mapping, we express the partition function as a path integral over Grassmann fields,

$$Z = \int \mathcal{D}\psi \mathcal{D}\bar{\psi} \exp(-S), \quad (2.6)$$

where  $S$  is the Euclidean action for  $\tilde{H}$ :

$$S = \int_\tau \sum_n [\bar{\psi}_1(n) \partial_\tau \psi_1(n) + \bar{\psi}_2(n) \partial_\tau \psi_2(n)] + \tilde{H}(\bar{\psi}, \psi). \quad (2.7)$$

Reinterpreting imaginary time as a spatial coordinate,  $\tau \rightarrow x$ , the action  $S$  can be viewed as a 2D Hamiltonian of chiral fermions, denoted  $H_{2D}$ . To bring it into a canonical form, we define new right- and left-moving fermion fields

$$\psi_{Rn} = (-1)^n \psi_1(n), \quad \psi_{Ln} = (-1)^n \psi_2(n), \quad (2.8)$$

$$\psi_{Rn}^\dagger = i(-1)^n \bar{\psi}_1(n), \quad \psi_{Ln}^\dagger = -i(-1)^n \bar{\psi}_2(n). \quad (2.9)$$

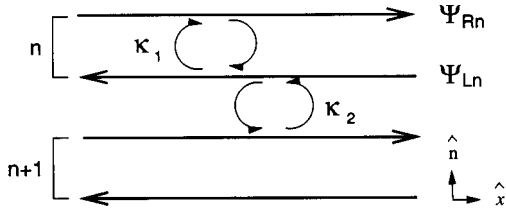


FIG. 2. A pictorial representation of the chiral fermion Hamiltonian (2.10). Neighboring chiral modes, propagating in the direction of the arrows, are coupled via tunneling matrix elements  $\kappa_i$ .

In terms of these the action becomes

$$H_{2D} = \int dx \sum_n [\psi_{Rn}^\dagger (i\partial_x) \psi_{Rn} + \psi_{Ln}^\dagger (-i\partial_x) \psi_{Ln} + \kappa_1 (\psi_{Rn}^\dagger \psi_{Ln} + \psi_{Ln}^\dagger \psi_{Rn}) + \kappa_2 (\psi_{Rn}^\dagger \psi_{Ln+1} + \psi_{Ln+1}^\dagger \psi_{Rn})]. \quad (2.10)$$

This Hamiltonian has a simple pictorial representation in terms of 1D right- and left-moving fermion fields, coupled together by hopping strengths  $\kappa_1$  and  $\kappa_2$ , as depicted in Fig. 2. The model closely resembles an anisotropic version of the Chalker-Coddington network model.<sup>3</sup> In the next section we describe a lattice version, appropriate for numerical simulations.

In the absence of disorder, with  $\kappa_1$  and  $\kappa_2$  constant,  $H_{2D}$  can be easily diagonalized by transforming to momentum space. The energy eigenvalues satisfy

$$E^2 = p_x^2 + \kappa_1^2 + \kappa_2^2 + 2\kappa_1\kappa_2 \cos p, \quad (2.11)$$

with  $p_x$  the  $x$  component of momentum and  $p$  a transverse momentum in the range  $-\pi$  to  $\pi$ . The energy is a minimum when  $p = \pi$  and  $p_x = 0$ , and given by  $|E|_{\min} = \pm |\Delta|$ , with  $\Delta = \kappa_1 - \kappa_2$ . The pure Ising critical point occurs when  $\Delta = 0$ . For  $\Delta \neq 0$ , there are no zero energy eigenvalues of the 2D Hamiltonian. If a wave of energy  $E = 0$  is incident in the  $x$  direction, it will decay as  $\exp(-|\Delta|x)$ , since  $p_x = i\Delta$  is pure imaginary. The decay length  $\xi \sim |\Delta|^{-1}$  corresponds to the correlation length of the pure 2D Ising model. The critical exponent is  $\nu_{\text{pure}} = 1$  as expected.

With disorder, the tunneling amplitudes  $\kappa_i$  become random functions of position  $n$  and  $x$  and momentum is not a good quantum number. Nevertheless, at the Ising multicritical point (see Fig. 1), one expects the  $E = 0$  states of  $H_{2D}$  to be *extended*, corresponding to an infinite correlation length. Away from criticality, one anticipates *localized* electronic states at  $E = 0$ , rather than a gap as in the pure case.

### III. NETWORK MODEL

In pioneering work, Chalker and Coddington<sup>3</sup> introduced a network model to study numerically the transition between IQHE plateaus. This model is essentially a lattice version of a chiral fermion Hamiltonian, similar Eq. (2.10). The model consists of links and nodes, as depicted in Fig. 3. On each link there is a complex amplitude representing the fermion

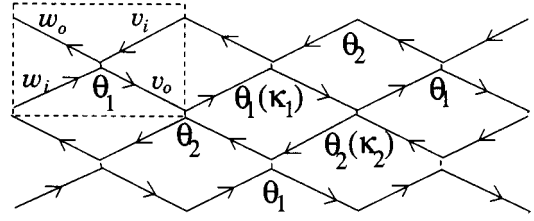


FIG. 3. Representation of network model with width  $L = 4$  and length  $N = 3$ . The arrows indicate the direction of wave propagation along links. The parameters  $\theta_i$  specify scattering at the nodes.

(electron) wave function. At the nodes, two incoming wave functions scatter into two outgoing ones, conserving probability. The nodes are specified by an  $S$  matrix. In the original network model,<sup>3</sup> the complex amplitudes acquired a random phase factor upon propagating along a given link, corresponding physically to a (random) magnetic flux through plaquettes.

On physical grounds, it is clear that a very similar network model should suffice for describing the propagation of  $E = 0$  waves of the Hamiltonian (2.10). In the appropriate network model, the tunneling amplitudes  $\kappa_i$  are replaced by node parameters. Since we are interested in  $E = 0$ , there are *no* phase factors associated with the links themselves. The network model is specified by a transfer matrix  $T$ , taken, say, in the horizontal direction in Fig. 3. This matrix is decomposed into a product of matrices  $M_j$ , representing columns of the network, with  $j$  running from 1 to  $N$ , the length of the network. Each matrix  $M_j$  is a product of two matrices  $M_j = A_j(\theta_1)B_j(\theta_2)$ , representing two adjacent nodes in Fig. 3. The two node parameters  $\theta_1$  and  $\theta_2$  correspond to the two hopping coefficients  $\kappa_1$  and  $\kappa_2$ .

The matrix representing tunneling at a given node is constructed to conserve the current or, equivalently, the  $U(1)$  charge. Following Chalker and Coddington,<sup>3</sup> the node in the dotted box in Fig. 3 is written as

$$\begin{pmatrix} w_{\text{out}} \\ w_{\text{in}} \end{pmatrix} = \begin{pmatrix} \cosh \theta_1 & \sinh \theta_1 \\ \sinh \theta_1 & \cosh \theta_1 \end{pmatrix} \begin{pmatrix} v_{\text{in}} \\ v_{\text{out}} \end{pmatrix}.$$

By construction, this matrix conserves the current,  $|w_{\text{in}}|^2 + |v_{\text{in}}|^2 = |w_{\text{out}}|^2 + |v_{\text{out}}|^2$ . Moreover, an incident wave, say,  $w_{\text{in}}$ , is backscattered into  $w_{\text{out}}$  with probability  $\tanh^2(\theta_1)$ . Since this tunneling probability is proportional to  $\kappa_1^2$  in the 2D Hamiltonian (2.10), we make the identification

$$\tanh(\theta_i) \leftrightarrow \kappa_i. \quad (3.1)$$

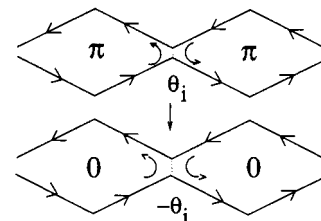


FIG. 4. A sign change in a node parameter  $\theta$  effectively changes by  $\pi$  the flux penetrating the two neighboring plaquettes.

Although the Hamiltonian (2.10) is intrinsically anisotropic, the network model can be made invariant<sup>3</sup> under a  $\pi/2$  spatial rotation by choosing  $\sinh(\theta_1)\sinh(\theta_2)=1$ , at successive nodes.

It is instructive to briefly consider the pure network model, with constant node parameters. In this case, the transfer matrix can be diagonalized in momentum space. For a

network with length  $N$  and width  $L$ , the total transfer matrix is  $T=M_0^N$ , with  $M_0$  an  $L\times L$  matrix. Due to translational invariance, the eigenvalues of  $M_0$ , and hence  $T$ , can be labeled by a transverse momentum  $p$ . We denote these as  $\lambda(p)$ . For a given transverse momentum  $p$ , these follow as eigenvalues of a simple  $2\times 2$  matrix:

$$\begin{pmatrix} \cosh\theta_1\cosh\theta_2 + \sinh\theta_1\sinh\theta_2e^{ip} & \sinh\theta_1\cosh\theta_2 + \cosh\theta_1\sinh\theta_2e^{ip} \\ \sinh\theta_1\cosh\theta_2 + \cosh\theta_1\sinh\theta_2e^{-ip} & \cosh\theta_1\cosh\theta_2 + \sinh\theta_1\sinh\theta_2e^{-ip} \end{pmatrix}.$$

One finds

$$\lambda_{\pm}(p) = A \pm \sqrt{A^2 - 1}, \quad (3.2)$$

with

$$A = \cosh(\theta_1 - \theta_2) + \sinh(\theta_1)\sinh(\theta_2)[1 + \cos(p)]. \quad (3.3)$$

As before, at the pure Ising critical point a nondecaying mode is expected. Since the eigenvalues of the total transfer matrix are  $\lambda^N$ , this is only possible if  $|\lambda|^2=1$ . This requires  $p=\pi$  and  $\theta_1=\theta_2$ , the expected condition for Ising criticality. Specializing to  $p=\pi$  and the isotropic case, with  $\sinh(\theta_1)\sinh(\theta_2)=1$ , the eigenvalues take the simple form

$$\lambda_{\pm} = \frac{1}{\lambda_{\mp}} = \frac{1+\Delta}{1-\Delta}, \quad (3.4)$$

with  $\Delta$  measuring the ‘‘distance’’ to the critical point:

$$\Delta = \tanh(\theta_1) - \tanh(\theta_2). \quad (3.5)$$

These eigenvalues describe the slowest decay of  $T\sim\lambda^N$ . The Ising correlation length follows as  $\xi=1/\ln(\lambda_+)$ , and as expected varies as  $\xi\sim 1/|\Delta|$  upon approaching the critical point,  $\Delta\rightarrow 0$ .

We now incorporate randomness. Due to the identification (3.1), a change in *sign* of the Ising exchange, corresponds to a sign change of a node parameter  $\theta_i$  in the network model. Thus the random-bond Ising model corresponds to a network model in which the *sign* of the node parameters is random. To be specific, we choose the *magnitude* of the node parameters to be constants  $\theta_1$  and  $\theta_2$ , satisfying the isotropy condition  $\sinh(\theta_1)\sinh(\theta_2)=1$ . The *sign* of  $\theta$  at each node is chosen randomly, being negative with probability  $W$  and positive with probability  $1-W$ . The random network model we consider is thus characterized by two parameters:  $\Delta$ , which measures the distance from criticality in the pure model, and  $W$  the disorder strength.

This model differs in symmetry from the original Chalker-Coddington network model,<sup>3</sup> in which random fluxes were present through each plaquette, reflecting the breaking of time-reversal invariance by the magnetic field in the QHE. In the present case, there are no random phase factors. However, in the pure model with all node parameters positive, the fermion amplitude picks up a minus sign upon encircling any elementary plaquette, equivalent to a uniform

flux  $\pi$  through each plaquette. Moreover, a sign change of a node parameter, changes the flux through two neighboring plaquettes by  $\pi$ , as depicted in Fig. 4.

Under the Ising duality transformation,  $\Delta\rightarrow -\Delta$ . Thus the  $\Delta=0$  line should correspond to the Ising ferromagnetic to paramagnetic phase boundary, depicted in Fig. 1. Increasing the randomness  $W$ , with  $\Delta=0$ , corresponds to moving along this phase boundary away from the pure Ising critical point. Based on Fig. 1, we expect the Ising multicritical point to correspond to some critical disorder strength  $W_c$ . Numerical simulations, described in the next section, indeed support this scenario. The scaling axis along the phase boundary corresponds to varying  $W$  with  $\Delta=0$ , whereas the Nishimori line corresponds to the line  $W=W_c$ .

For  $W>W_c$  and  $\Delta=0$ , one expects the network model to remain critical, due to duality symmetry. However, it is unclear what this regime corresponds to in the original lattice Ising model (1.1). It is conceivable that increasing  $W$  beyond  $W_c$  (at  $\Delta=0$ ) corresponds to moving along the low-temperature part of the phase boundary in Fig. 1, arriving at the  $T=0$  fixed point at the maximum disorder strength,  $W_{\max}=1/2$ . However, this interpretation is a bit problematic since  $W=1/2$  is ‘‘halfway’’ between the ferromagnet and antiferromagnet, and naively corresponds to  $p=1/2$  in Fig. 1. Perhaps the time continuum limit taken in Eq. (2.1), does *not* give a faithful representation of the lattice Ising model (1.1) for  $W>W_c$ .

#### IV. RESULTS

The transfer matrix  $T$  of the random network model can be computed numerically, following the work of Chalker<sup>3</sup> and others.<sup>11-13</sup> We have studied strips of width  $L$  ranging from  $L=16$  up to  $L=128$ . Ensemble averaging is performed by taking very long strips, with length  $N$  up to  $10^5$ . Of the  $L$  eigenvalues of  $T_N$ , denoted  $\lambda_i$ ,  $L/2$  are greater than 1, corresponding to exponentially growing solutions, and the others are less than 1, decaying to zero with increasing  $N$ . Due to the (statistical) parity of the system, these come in pairs,  $\lambda_i=\exp(\pm N\gamma_i)$ , where  $i=1,2,\dots,L/2$  and all the  $\gamma_i^s$  are positive. Of interest is the smallest,  $\gamma_{\min}$ , corresponding to the most slowly decaying mode. From this one extracts the correlation length as

$$\xi_L = \frac{1}{\gamma_{\min}}. \quad (4.1)$$

In order to extrapolate to the thermodynamic limit,  $L \rightarrow \infty$ , it is convenient to consider the dimensionless ratio,

$$\Lambda_L(\Delta, W) \equiv \frac{L}{\xi_L}, \quad (4.2)$$

which is a function of the two control parameters  $W$  and  $\Delta$ . Away from criticality ( $\Delta \neq 0$ ),  $\xi_{L=\infty}$  is finite, and so this ratio should grow and diverge as  $L \rightarrow \infty$ . Representative data are shown in Fig. 7, where  $\Lambda_L$  is plotted versus  $\Delta$  for weak randomness  $W=0.075$ , at various different system sizes. At the pure Ising critical point  $\Delta=W=0$ , the ratio  $\Lambda_L$  is found to vanish identically even for *finite*  $L$ , due to the propagating mode with transverse momentum  $p=\pi$ , described by Eq. (3.2). At a random critical point, one expects that  $\Lambda_L$  will approach a finite constant in the thermodynamic limit, reflecting the infinite correlation length.

In Fig. 5 we show data for  $\Lambda_L$  versus disorder strength  $W$ , along the phase boundary,  $\Delta=0$ , at four different system widths  $L$ . Although there is significant variation with  $L$ , particularly for the smaller sizes, there appear to be two distinct regimes separated by a peak. For the largest width ( $L=128$ ) the peak occurs at a disorder strength  $W_c \approx 0.08$ . For  $W < W_c$  the ratio  $\Lambda_L$  drops rapidly towards zero, the value at the pure Ising critical point. For strong disorder  $W > W_c$  the ratio appears to be settling down towards a constant of order  $1/2$  at large  $L$ . This presumably corresponds to a strong disorder critical point. Right at the critical disorder strength  $W=W_c$ ,  $\Lambda_L$  is increasing slowly with  $L$ , and presumably eventually saturates. We thus identify the point ( $\Delta=0$ ,  $W=W_c$ ) with the random Ising multicritical point (see Fig. 1).

This identification can be confirmed by extracting critical exponents, and comparing with the values obtained by Singh

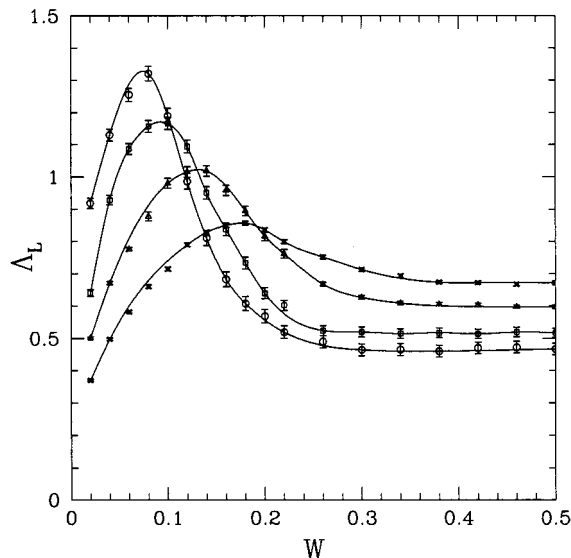


FIG. 5. Dimensionless ratio  $\Lambda_L$  vs disorder strength  $W$  along the phase boundary  $\Delta=0$  for four different system widths:  $L=16(\times)$ ,  $L=32(\triangle)$ ,  $L=64(\square)$ , and  $L=128(\circ)$ .

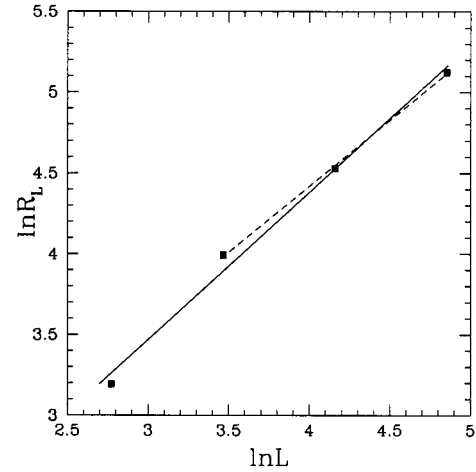


FIG. 6. Curvatures  $R_L$  of parabolic fits to the peaks in Fig. 5, vs system width  $L$  on a doubly logarithmic plot. From scaling, the slope gives an estimate for the critical exponent  $2/\nu_p$ .

and Adler<sup>4</sup> at the Ising multicritical point. Unfortunately, precise values are difficult to extract due to the rather severe finite size effects, evident in Fig. 5. These are due (in part) to the small value of  $W_c$ : With  $W_c \approx 0.08$ , the typical nearest distance between two nodes with negative node parameters,  $\theta_i$ , is roughly 4 times the network lattice spacing.

Consider first the critical exponent corresponding to the scaling axis along the phase boundary, denoted  $\nu_p$ . A natural finite-size scaling *ansatz* for  $\Lambda_L$  takes the form

$$\Lambda_L(\Delta=0, W) = f[L^{1/\nu_p}(W - W_c)], \quad (4.3)$$

for large  $L$  and  $W \rightarrow W_c$ . This form predicts that peaks in  $\Lambda_L(W)$  around  $W_c$  should sharpen up with a width vanishing as  $\delta W \sim L^{-1/\nu_p}$ . The data in Fig. 5 are consistent with this trend, showing narrower peaks for larger  $L$ . To obtain a rough estimate for the exponent  $\nu_p$ , we fit the peaks to a parabola. Denoting the curvatures of the parabolas as  $R_L$ , scaling predicts  $R_L \sim L^{2/\nu_p}$ . In Fig. 6 we plot  $\log(R_L)$  versus  $\log(L)$  and extract the exponent  $2/\nu_p$  as the slope of a fitted straight line. Fitting all four points gives an estimate  $\nu_p \sim 2.2$ . However, the  $\chi^2$  per data points decreases an order of magnitude if the smallest size  $L=16$  is excluded, which gives (dotted line in Fig. 6)  $\nu_p \sim 2.45$ . Thus we estimate  $\nu_p \approx 2.4$ , with a large error bar  $\pm 0.3$ .

The critical exponent along the Nishimori line can be extracted by sitting at  $W_c$  and tuning  $\Delta$  away from zero. In this case, finite-size scaling implies that

$$\Lambda_L(\Delta, W=W_c) = F[L^{1/\nu} \Delta]. \quad (4.4)$$

The raw data for  $\Lambda_L(\Delta, W_c)$  versus  $\Delta$  are shown in Fig. 7. As expected, away from the multicritical point at  $\Delta=0$ , the ratio  $\Lambda_L$  grows with  $L$ , indicative of a finite correlation length. In Fig. 8 these data for  $\Delta < 1/2$  are replotted, rescaling the horizontal axis by  $L^{1/\nu}$ . Based on the quality of the data collapse, we estimate  $\nu \approx 4/3$  with error bars  $\pm 0.1$ .

Our estimates for the exponents compare favorably with those obtained by Singh and Adler<sup>4</sup>:  $\nu = 1.32 \pm 0.08$  and

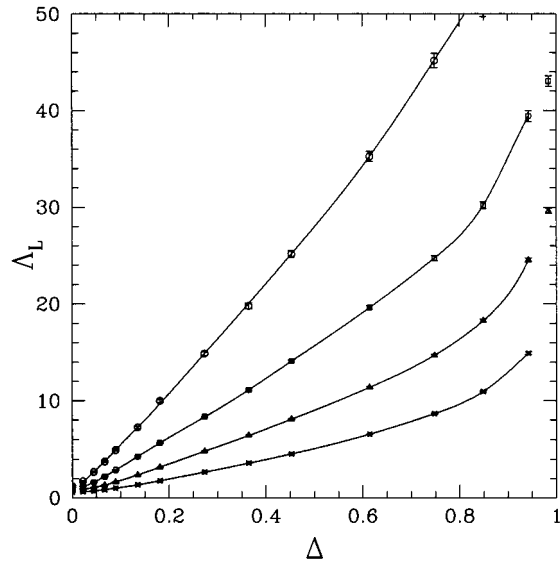


FIG. 7. Dimensionless ratio  $\Lambda_L = L/\xi_L$  plotted vs  $\Delta$  at disorder strength  $W=0.075$  for four different system sizes:  $L=16$  ( $\times$ ),  $L=32$  ( $\Delta$ ),  $L=64$  ( $\square$ ), and  $L=128$  ( $\circ$ ).

$\nu_p \approx (5/3)\nu \approx 2.2$ . This agreement gives one confidence that the peak in Fig. 5 does indeed correspond to the random Ising multicritical point.

In addition to the multicritical point, we have tried to analyze the behavior at maximal disorder strength  $W=1/2$ . As discussed earlier, it is unclear whether or not this point corresponds to the  $T=0$  fixed point at  $p=p_c$  in the random-bond Ising model (Fig. 1). Unfortunately, at  $W=1/2$  we are even more severely plagued by finite-size effects as  $\Delta$  is varied. Specifically, the correlation length tends to remain very long, even well away from criticality, with  $\Delta \rightarrow 1$ . In this limit, the fermions tend to become localized around plaquettes on one sublattice. But with  $W=1/2$ , half of the plaquettes have zero flux, and can support ( $E=0$ ) states circling around them. For  $1-\Delta$  small, these states will be weakly coupled via tunneling, and may tend to percolate out to rather long scales. At this stage, we cannot conclude anything definite about the critical behavior of the network model at strong disorder.

## V. CONCLUSION

To summarize, we have shown that the 2D random bond Ising model can be fruitfully mapped onto a network model for chiral fermions. The network model is similar to the original Chalker-Coddington model<sup>3</sup> used to study IQHE

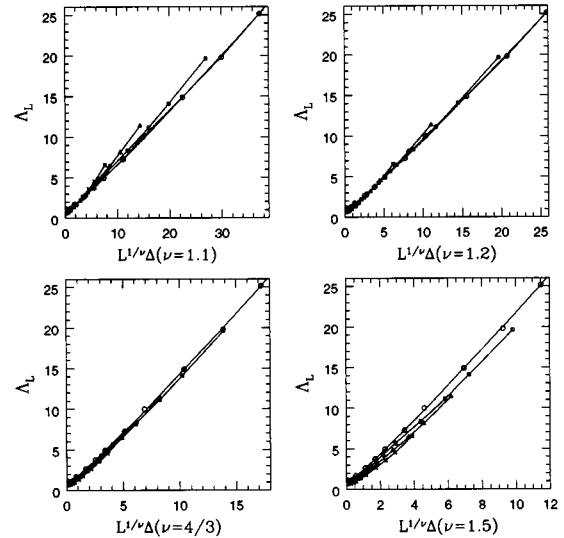


FIG. 8. Scaling collapse of the data from Fig. 7 with  $\Delta < 1/2$  for four different exponent values:  $\nu=1.1$ ,  $1.2$ ,  $4/3$ , and  $1.5$ .

plateau transitions, but with different symmetry. Specifically, the model has node parameters with random signs, rather than random fluxes through plaquettes. The network model has been used to study the novel random multicritical point which exists on the Ising ferromagnetic to paramagnetic phase boundary. By implementing a numerical transfer matrix approach, estimates for the associated critical exponents have been extracted, which are consistent with those obtained by Singh and Adler<sup>4</sup> from high-temperature series. The critical exponents are quite different from those at the IQHE plateau transition, indicating different universality classes, not surprising in view of the symmetry differences between the two models.

What are the prospects for an analytic treatment of the random Ising multicritical point? Being in two dimensions, one might hope that powerful constraints from conformal invariance would be helpful. Analytic approaches to the IQHE plateau transition have been impeded by the absence of critical behavior in ensemble-averaged single-particle Green's functions. The situation might be simpler at the Ising multicritical point, though, since critical properties are probably present in average single-fermion correlators.

## ACKNOWLEDGMENTS

It is a pleasure to acknowledge fruitful conversations with Leon Balents, Daniel Fisher, Derek Lee, Dongzi Liu, and Andreas Ludwig. We are grateful to the National Science Foundation for support, under Grant Nos. PHY94-07194, DMR-9400142, and DMR-9528578.

<sup>1</sup>See Claude Itzykson and Jean-Michel Drouffe, *Statistical Field Theory* (Cambridge University Press, Cambridge, 1989), Vols. 1 and 2, and references therein.

<sup>2</sup>For a recent see B. Huckestein, *Rev. Mod. Phys.* **67**, 357 (1995).

<sup>3</sup>J. T. Chalker and P. D. Coddington, *J. Phys. C* **21**, 2665 (1988).

<sup>4</sup>R. R. P. Singh and J. Adler, *Phys. Rev. B* **54**, 364 (1996).

<sup>5</sup>See K. Binder and A. P. Young, *Rev. Mod. Phys.* **58**, 801 (1986), and references therein.

<sup>6</sup>A. P. Young and B. W. Southern, *J. Phys. C* **10**, 2179 (1977); R. Maynard and R. Rammal, *J. Phys. (Paris) Lett.* **43**, L347 (1982); Y. Ozeki and H. Nishimori, *J. Phys. Soc. Jpn.* **56**, 1568 (1987);

- 56**, 3265 (1987); W. L. McMillan, Phys. Rev. B **29**, 4026 (1986).
- <sup>7</sup>Y. Ueno and Y. Ozeki, J. Stat. Phys. **64**, 227 (1991); H. Kitatani and T. Oguchi, J. Phys. Soc. Jpn. **59**, 3823 (1990); **61**, 1598 (1992); Y. Ozeki, *ibid.* **59**, 3531 (1990).
- <sup>8</sup>P. LeDoussal and A. B. Harris, Phys. Rev. Lett. **61**, 625 (1988).
- <sup>9</sup>H. Nishimori, Prog. Theor. Phys. **66**, 1169 (1981).
- <sup>10</sup>R. Shankar, Phys. Rev. Lett. **58**, 2466 (1987).
- <sup>11</sup>Dung-Hai Lee, Ziqiang Wang, and Steven Kivelson, Phys. Rev. Lett. **70**, 4130 (1993).
- <sup>12</sup>Dongzi Liu and Das Sarma, Phys. Rev. B **49**, 2677 (1993).
- <sup>13</sup>D. K. K. Lee and J. T. Chalker, Phys. Rev. Lett. **72**, 1510 (1994).